Coherent states in projected Hilbert spaces

P. D. Drummond and M. D. Reid

Phys. Rev. A **94**, 063851 — Published 23 December 2016

DOI: 10.1103/PhysRevA.94.063851

Coherent states in projected Hilbert spaces

P. D. Drummond and M. D. Reid
Centre for Quantum and Optical Science, Swinburne University of Technology, Melbourne 3122 Australia

Coherent states in a projected Hilbert space have many useful properties. When there are conserved quantities, a representation of the entire Hilbert space is not necessary. The same issue arises when conditional observations are made with post-selected measurement results. In these cases, only a part of the Hilbert space needs to be represented, and one can define this restriction by way of a projection operator. Here coherent state bases and normally-ordered phase-space representations are introduced for treating such projected Hilbert spaces, including existence theorems and dynamical equations. These techniques are very useful in studying novel optical or microwave integrated photonic quantum technologies, such as boson sampling or Josephson quantum computers. In these cases states become strongly restricted due to inputs, nonlinearities or conditional measurements. This paper focuses on coherent phase states, which have especially simple properties. Practical applications are reported on calculating recurrences in anharmonic oscillators, the effects of arbitrary phase-noise on Schrödinger cat fringe visibility, and on boson sampling interferometry for large numbers of modes.

I. INTRODUCTION

Coherent states are a widely used concept in quantum physics. Originally introduced by Schrödinger[1], and extended by Bargmann[2] and Glauber[3], these are often applied to quantum optics and quantum technologies. The generalized P-representation [4, 5] makes extensive use of these states: it is a complete phase-space representation on multi-mode bosonic Hilbert space, which extends the Glauber-Sudarshan P-function [6, 7] by allowing non-singular distributions for any quantum state or density matrix. It can be utilized for both exact, analytic solutions, and stochastic simulations of dynamics[8–10]. It has a high degree of scalability, permitting exponentially large Hilbert space problems to be treated [11], as well as large occupation numbers [12].

Yet sometimes only part of the full Hilbert space is needed. There may only be occupation numbers of $(0, 1)$, or else conservation laws of energy, number or momentum may restrict the Hilbert space. For these physical problems, it is unnecessary to utilize states that form a basis for the whole Hilbert space, since only part of it is occupied. This type of problem can be treated using projected representations. An example of this is number conservation, which can lead to invariance under projection such that states with total numbers differing from N do not need to be represented.

To treat such restricted Hilbert spaces in bosonic cases, this paper introduces projected coherent states and corresponding phase-space representations where projections are included by redefining the coherent states. The resulting mappings are more focused and compact than with the full coherent basis. This approach includes a type of discrete coherent state, called a coherent phase states (CPS), which are cousins to the phase states of quantum optics [13, 14]. These allow a definition of a discrete P-function with similarities to the discrete Wigner function [15–17]. The utility of coherent phase states is that they satisfy operator identities almost identical to the full coherent states, thus allowing dynamical evolution to be calculated. They can be applied efficiently to photonic networks and boson sampling problems [18].

A projected phase-space technique can have a greater numerical efficiency, and lower sampling error, when the physically occupied Hilbert space is a small fraction of the Hilbert space. As an example of this, fermionic phase-space representations of the Hubbard model that include conservation laws result in improved numerical simulations [19]. In other cases where the total experimental density matrix $\hat{\rho}$ is not invariant under projection, one may still be interested in measurements only on a projected part of the density matrix. These are post-selected measurements, and are common in many quantum optics experiments [20–22].

The examples given here are all cases where the projectors commute with the number operator. A typical experimental protocol is the photonic Bell experiment, where all measurements yielding the vacuum state are projected out via post-selection [22, 23]. There are many other novel experimental technologies which combine growing exponential complexity with a restricted Hilbert space. A well-known case is "boson sampling" [24, 25], which has led to photonic waveguide experiments [26–29] and metrology proposals [30, 31]. Some of these ideas, originally in the optical domain, have also been extended to superconducting waveguide qubits [32], and are applicable to massive bosons as well.

Other quantum technologies, including arrays of optomechanical devices [33] and quantum gas microscopes for BEC systems [34], can operate in a similar regime. These systems have a combination of exponential complexity - making orthogonal basis techniques difficult to scale - together with restricted occupation numbers which makes projection techniques useful. This paper establishes the general foundations of this approach. Particular applications are treated elsewhere [18].

Section II introduces projected coherent states, together with coherent phase states. Differential and matrix identities are obtained in Section III. Section IV defines projected P-representations, which use the pro-

jected coherent states, and obtains existence theorems while Section V discusses applications to photonic networks, including an anharmonic example, phase decoherence in a Schrödinger Cat, and boson sampling experiments. Finally, Section VI gives the conclusions.

II. PROJECTED STATES

Coherent states have many uses in calculations in physics, and they are a complete basis. However, dealing with the complete Hilbert space is often not necessary. There can be restrictions and symmetries that limit the available states. Here, ways to define coherent states with projective restrictions are introduced. These still lead to a complete basis in the Hilbert sub-space of interest.

Projection operators on a Hilbert space can be applied to states, operators or to the density matrix. Suppose the projector is $\mathcal{P}$, defined so that $\mathcal{P}=\mathcal{P}^2$. If there are multiple projections $\mathcal{P}_j$, they are assumed to commute, so that their product $\mathcal{P}=\prod\mathcal{P}_j$ is a projector. Given a state $|\psi\rangle$, its projected versions will be written as $|\psi\rangle_{\mathcal{P}}=\mathcal{P}\,|\psi\rangle$. When there are normalization requirements, there is an additional scale factor, defined as needed. In this section, results are obtained for projection operators applied to coherent states.

A. Coherent states

Throughout this paper, an M mode system of bosons is treated with number states that are outer products of number states $|n_j\rangle_j$ for each mode, so that:

$$|n_1,\ldots,n_M\rangle\equiv\prod_{j=1}^{M}|n_j\rangle_j\ . \tag{2.1}$$

The coherent states $\|\boldsymbol{\alpha}\rangle$ and $|\boldsymbol{\alpha}\rangle$ are respectively the unnormalized and normalized eigenstate of annihilation operators $\hat{\mathbf{a}}=[\hat{a}_1,\ldots\hat{a}_M]$, with eigenvalues $\boldsymbol{\alpha}$. To prevent ambiguity, coherent states are labelled with greek letters $|\boldsymbol{\alpha}\rangle$, number states with roman letters $|\boldsymbol{n}\rangle$. The coherent state basis is conventionally written in terms of $\boldsymbol{\alpha}=[\alpha_1,\ldots\alpha_M]$, which is a complex vector of coherent amplitudes. In the multi-mode case, the unnormalized coherent state has the standard form of [2]:

$$\|\boldsymbol{\alpha}\rangle=\sum_{\mathbf{n}\geq 0}\prod_i\frac{\alpha_i^n}{\sqrt{n_i!}}|n_i\rangle_i=\sum_{\mathbf{n}\geq 0}\|\boldsymbol{\alpha}\rangle_{\mathbf{n}}\,. \tag{2.2}$$

where the state $\|\boldsymbol{\alpha}\rangle_{\mathbf{n}}$ is an unnormalized coherent state projected onto a fixed number $\boldsymbol{n}$, so that:

$$\|\boldsymbol{\alpha}\rangle_{\mathbf{n}}\equiv\prod_i\frac{\alpha_i^n}{\sqrt{n_i!}}|n_i\rangle_i\ . \tag{2.3}$$

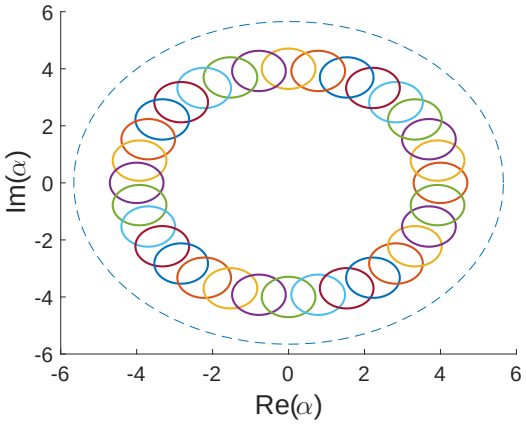

Figure 1. The coherent phase states for dimension $d=32$, with coherent radius of $\alpha=4$. The dotted line is the number state cut-off at a radius of $\sqrt{d}$. The colored circles are a circle of uncertainty for each coherent phase-state of radius $\Delta x=\Delta y=1/\sqrt{2}$. This is the Heisenberg uncertainty or standard deviation in a measurement of $\hat{x}=\left(\hat{a}+\hat{a}^\dagger\right)/2$ for a coherent state $|\alpha\rangle=|x+iy\rangle$.

For coherent states projected onto single number states, the following identities hold:

$$\begin{aligned}\hat{a}\,\|\alpha\rangle_n&=\alpha\,\|\alpha\rangle_{n-1}\ ,\\ \hat{a}^\dagger\,\|\alpha\rangle_n&=\frac{n+1}{\alpha}\,\|\alpha\rangle_{n+1}\,.\end{aligned} \tag{2.4}$$

The corresponding *normalized* coherent state is [35, 36]:

$$|\boldsymbol{\alpha}\rangle=g\,(\boldsymbol{\alpha})^{-1}\,\|\boldsymbol{\alpha}\rangle\ , \tag{2.5}$$

where $g\,(\boldsymbol{\alpha})=e^{|\boldsymbol{\alpha}|^2/2}=\sqrt{\langle\boldsymbol{\alpha}\,\|\boldsymbol{\alpha}\rangle}$ is the norm.

B. Projected coherent states

Next, consider a *projected* coherent basis. In the unnormalized case this is simply

$$\|\boldsymbol{\alpha}\rangle_{\mathcal{P}}=\mathcal{P}\,\|\boldsymbol{\alpha}\rangle\ . \tag{2.6}$$

For the normalized case, there is a modified normalization as well, so that in this case one can define:

$$|\boldsymbol{\alpha}\rangle_{\mathcal{P}}=g_{\mathcal{P}}^{-1}\,\|\boldsymbol{\alpha}\rangle_{\mathcal{P}}\ , \tag{2.7}$$

where $g_{\mathcal{P}}=g_{\mathcal{P}}\,(\boldsymbol{\alpha})=\sqrt{\langle\boldsymbol{\alpha}\|\,\mathcal{P}\,\|\boldsymbol{\alpha}\rangle}$. The abbreviated form $g_{\mathcal{P}}$ for the normalization will be used if there is no ambiguity. This is not just an outer product, but rather is a linear combination of all possible number states $|\boldsymbol{n}\rangle$ that satisfy the projection requirements, with coefficients given by the appropriate coherent amplitudes.

As one example of this, coherent phase states (CPS) will be introduced. These are a complete, linearly independent set of projected coherent states which are complementary to a set of number states, as illustrated in

Fig (1). In general, projected states can have both coherence properties and a conservation law. Such properties are useful in describing Bose Einstein condensates which have long range coherence, but a fixed or bounded number.

C. Number projected coherent states

Many common physical systems have a restricted range of bosonic occupation numbers n_i, such that $\boldsymbol{n} \in S$, where S is the set of physically allowed values. As one example, the total boson number may be constrained so that $\sum n_i = N$. This can occur due to number conservation combined with a number-sensitive preparation or post-selection. If there are dissipative losses, the total number may have an upper bound so that $\sum n_i \leq N_m$.

To treat this, define $\mathcal{P} \equiv \mathcal{N}$ as the projector onto the number states with $\boldsymbol{n} \in S$. This is an identity operator in the projected space, so that:

$$\hat{I}_{\mathcal{N}} = \mathcal{N} = \sum_{\boldsymbol{n}\in S} |\boldsymbol{n}\rangle \langle \boldsymbol{n}| . \tag{2.8}$$

The unnormalized projected state is :

$$\|\boldsymbol{\alpha}\rangle_{\mathcal{N}} = \mathcal{N} \|\boldsymbol{\alpha}\rangle = \sum_{\boldsymbol{n}\in S} \prod_i \frac{\alpha_i^{n_i}}{\sqrt{n_i!}} |n_1, \ldots, n_M\rangle . \tag{2.9}$$

The normalized projected coherent state is then defined as in (2.7), where the normalization is:

$$g_{\mathcal{N}}(\boldsymbol{\alpha}) = \sqrt{\sum_{\boldsymbol{n}\in S} \prod_i \frac{|\alpha_i|^{2n_i}}{n_i!}} . \tag{2.10}$$

For the single-mode case with a number cutoff projection such that $n \leq N_m = n_m$, the normalization is proportional to an upper incomplete gamma function [37],

$$g_{\mathcal{N}}(\alpha) = \sqrt{\frac{1}{n_m!} e^{|\alpha|^2} \Gamma(1 + n_m, |\alpha|^2)} . \tag{2.11}$$

In cases of number projections, invariant observables of form $\hat{O} = \hat{a}_m^\dagger \cdots \hat{a}_n$ are usually of most interest. These have an equal number of annihilation and creation operators, and are called *number-conserving observables*.

When both the projectors and observables are number-conserving, it follows that the observables commute with the projectors, as they have a complete set of simultaneous eigenstates, i.e., for number conserving observables,

$$\hat{a}_m^\dagger \cdots \hat{a}_n \mathcal{N} = \mathcal{N} \hat{a}_m^\dagger \cdots \hat{a}_n . \tag{2.12}$$

In some, but not all cases, invariant observables have the number states as eigenstates, so that $\hat{O}|\mathbf{n}\rangle = O_{\mathbf{n}} |\mathbf{n}\rangle$.

D. Qudit bosonic coherent states

A qudit coherent state is defined to have a range of occupation numbers n_i in *each* mode, such that $n_i \in s$, where s is a set of d allowed number values. This type of finite dimensional qudit [38] has a projector denoted $\mathcal{Q}$.

The projected identity operator factorizes, so that:

$$\hat{I}_{\mathcal{Q}} = \mathcal{Q} = \prod_j \left[\sum_{n_j \in s} |n_j\rangle \langle n_j|_j \right] . \tag{2.13}$$

An alternative approach in this situation would be to define $SU(d)$ coherent states for qudits. These have different combinatorial coefficients [39–43]. However, this is a Lie group symmetry which is more suitable for spins rather than for boson operator identities, due to the different operator algebras in the two cases.

Binary qubits occur for for $d = 2$, where the projected coherent states are isomorphic to $SU(2)$ coherent states. The simplest case has $n = 0, 1$; so that only zero and one boson states are included, which makes this useful for Bell inequalities, quantum computers or boson sampling.

For general qudits, the single mode case is identical to the previous section. In the multi-mode case, the unnormalized state factorizes so that:

$$\|\boldsymbol{\alpha}\rangle_{\mathcal{Q}} = \mathcal{Q} \|\boldsymbol{\alpha}\rangle = \prod_i \left[\sum_{n_i \in s} \frac{\alpha_i^{n_i}}{\sqrt{n_i!}} |n_i\rangle_i \right] . \tag{2.14}$$

The normalized multi-mode qudit coherent state is given in (2.7), with normalization $g_{\mathcal{Q}}(\boldsymbol{\alpha}) = \prod_i g_{\mathcal{Q}}(\alpha_i)$, where

$$g_{\mathcal{Q}}(\alpha) = \sqrt{\sum_{n\in s} \frac{(\alpha^* \alpha)^n}{n!}} . \tag{2.15}$$

Here $g_{\mathcal{Q}}(\alpha)$ is given analytically by (2.11) in the number cut-off case with $n_i \leq n_m$. The approximation $g_{\mathcal{Q}}(\boldsymbol{\alpha}) \approx e^{|\boldsymbol{\alpha}|^2/2}$ is valid for number cut-off qudit projections such that $|\alpha_i|^2 \ll d$.

The single-mode qudit projection operator can be rewritten in terms of coherent number states as:

$$\hat{I}_{\mathcal{Q}} = \sum_{n\in s} g_n^{-2} \|\alpha\rangle_n \langle \alpha\|_n , \tag{2.16}$$

where the normalization coefficient of a coherent state projected onto a single number state is:

$$g_n = \sqrt{|\alpha|^{2n}/n!} . \tag{2.17}$$

Here g_n^2 has a well-known role in probability theory: combined with an overall normalization of $e^{-|\alpha|^2}$, it is the probability of observing a number n in a Poisson distribution with mean $|\alpha|^2$. For large $|\alpha|^2$ this is approximately normal, with equal mean and variance, $\mu = \sigma^2 = |\alpha|^2$. Hence, in the large $|\alpha|$ limit,

$$g_n^2 \approx \frac{1}{\sqrt{2\pi |\alpha|^2}} e^{|\alpha|^2 - (n/|\alpha| - |\alpha|)^2/2} . \tag{2.18}$$

This Gaussian cutoff for $n/|\alpha|^2 > 1$ is the main reason why even a projected coherent state can still maintain many of the useful properties of the full set. This is rapidly convergent, so in a numerical calculation in which an initial coherent state is projected, the calculations can be easily repeated with a larger cutoff to check that no significant errors are introduced.

E. Coherent phase states

Qudit number projections over a contiguous interval $n_0 \leq n_i \leq n_m$ have many interesting properties. It is useful to consider coherent state amplitudes with discrete phases, so $\alpha^{(q)} \equiv \alpha \exp(iq\phi)$, for $q = 0, \ldots d-1$, where

$$\phi \equiv \frac{2\pi}{d} \,. \tag{2.19}$$

Here $\alpha^{(q)}$ is defined relative to a reference amplitude α. This gives a projected basis with coherent amplitudes having a fixed intensity, distributed in a circle on the complex plane as shown in Fig (1), which can be termed *coherent phase states* (CPS). These types of projected coherent states are similar to the quantum phase states [13, 14], which have a well-defined phase. The simplest has the ground state included so that $n_0 = 0$.

They have the useful property that discrete Fourier transform relations are available for a coherent qudit with $d = 1 + n_m - n_0$. A circular basis results in an invertible mapping between coherent phase and number states for $n_0 \leq n \leq n_m$, since it can be written in the form:

$$\left\| \alpha^{(q)} \right\rangle_{\mathcal{Q}} = \sum_{n=n_0}^{n_m} e^{iqn\phi} \left\| \alpha \right\rangle_n \tag{2.20}$$

which, from the discrete Fourier transform theorem, has the corresponding inverse relation that:

$$\left\| \alpha \right\rangle_n = \frac{1}{d} \sum_{q=0}^{d-1} e^{-iqn\phi} \left\| \alpha^{(q)} \right\rangle_{\mathcal{Q}} \,. \tag{2.21}$$

There is a corresponding multimode coherent phase state, written as:

$$\left\| \boldsymbol{\alpha}^{(\boldsymbol{q})} \right\rangle_{\mathcal{Q}} = \prod_{j=1}^{M} \left\| \alpha^{(q_j)} \right\rangle_{\mathcal{Q}} \,, \tag{2.22}$$

with a normalized form

$$\left| \boldsymbol{\alpha}^{(q)} \right\rangle_{\mathcal{Q}} = g_{\mathcal{Q}}^{-1} \left\| \boldsymbol{\alpha}^{(\boldsymbol{q})} \right\rangle_{\mathcal{Q}} \,. \tag{2.23}$$

This basis is familiar with qubits having $d = 2$ and $n_0 = 0$, where $g_{\mathcal{Q}} = \sqrt{1 + |\alpha|^2}$, and one has:

$$\left| \alpha^{(0,1)} \right\rangle_{\mathcal{Q}} = g_{\mathcal{Q}}^{-1} \left[|0\rangle \pm \alpha \, |1\rangle \right] \,. \tag{2.24}$$

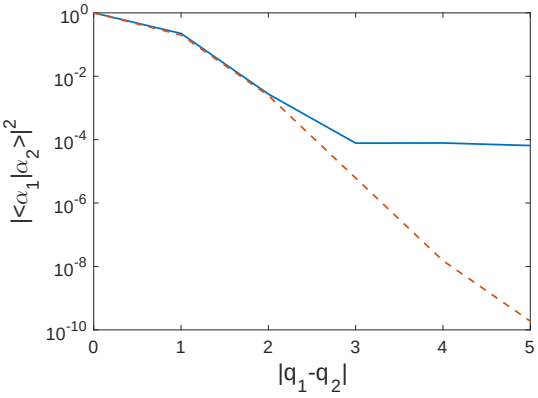

Figure 2. Orthogonality versus phase difference of coherent phase states $|\alpha_i\rangle = \left|\alpha^{(q_i)}\right\rangle$ for $n_0 = 0$ and $n_m = 11$, with $|\alpha|^2 = d/2 = 6$. Solid line gives the degree of orthogonality of two coherent phase states with distance $|q_1 - q_2|$, dotted line the orthogonality of two standard coherent states.

The coherent phase states are linearly independent, but not completely orthogonal. In general,

$$\left\langle \alpha^{(q_1)} \right| \left. \alpha^{(q_2)} \right\rangle_{\mathcal{Q}} = M_{q_1,q_2} \,, \tag{2.25}$$

where the inner product of two coherent phase states is given by:

$$M_{q_1,q_2} = g_{\mathcal{Q}}^{-2} \sum_{n=n_0}^{n_m} e^{i(q_2-q_1)n\phi} \frac{|\alpha|^{2n}}{n!} \,. \tag{2.26}$$

With the choice that $|\alpha|^2 = (n_0 + d/2)$, states with $q_1 \neq q_2$ are orthogonal for the qubit case, and approximately orthogonal in the general case, as shown in Fig (2).

Such states form a middle ground between the number states, which are orthogonal but lack coherence, and the coherent states which have coherence but are highly overcomplete. Changing the coherent radius $r = |\alpha|$ has no effect on the completeness of the mapping, but it does change the orthogonality, as shown in Fig (3).

A smaller radius gives closely spaced coherent amplitudes with reduced orthogonality for nearest neighbors, but this increases for widely separated phases. For a larger coherent radius the orthogonality at small phase separations is greater. However, for large radius *and* large phase separations, the orthogonality is reduced since the number cutoff has a strong effect in this limit.

F. Coherent phase expansions

Since coherent phase states comprise a complete basis in the projected subspace, it is possible to expand an arbitrary projected state $|\psi\rangle = \mathcal{P} \, |\psi\rangle$ using these states, just as with the full coherent basis [6]. This expansion

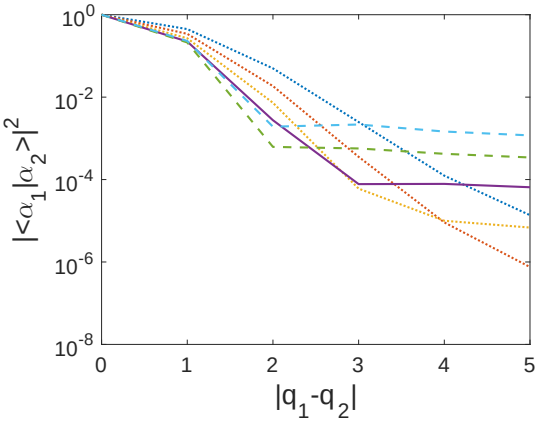

Figure 3. Orthogonality versus phase difference of coherent phase states $|\alpha_i\rangle = \left|\alpha^{(q_i)}\right\rangle$ for $n_0 = 0$ and $n_m = 11$, with $|\alpha|^2 = 3, 4, 5, 6, 7, 8$. The dotted lines have smaller radii with $|\alpha|^2 < 6$, with $|\alpha|^2 = 3$ the upper line. The solid line has $|\alpha|^2 = 6$. The dashed lines have larger radii, with $|\alpha|^2 = 8$ the upper line on the right.

can be written in a multimode case as:

$$|\psi\rangle = \sum_{\boldsymbol{q}} \psi_{\boldsymbol{q}} \left\|\boldsymbol{\alpha}^{(\boldsymbol{q})}\right\rangle_{\mathcal{Q}} . \tag{2.27}$$

Unlike the non-unique coherent state case, this expansion is unique, owing to the linear independence of the CPS basis. In the single-mode case, given a number state expansion $|\psi\rangle = \sum_{\boldsymbol{n}} \psi_{\boldsymbol{n}} |\boldsymbol{n}\rangle$, the CPS coefficients are:

$$\psi_{\boldsymbol{q}} = \sum_{\boldsymbol{n}} \psi_{\boldsymbol{n}} \prod_j \frac{\sqrt{n_j!}}{d\left(\alpha^{(q_j)}\right)^{n_j}} . \tag{2.28}$$

The expectation value of any observable $\hat{O}$ in a pure state is then given by:

$$\left\langle \hat{O} \right\rangle = \sum_{\vec{\boldsymbol{q}}} \psi^*_{\boldsymbol{q}} \psi_{\boldsymbol{q}'} \left\langle \boldsymbol{\alpha}^{(\boldsymbol{q})} \right\| \hat{O} \left\| \boldsymbol{\alpha}^{(\boldsymbol{q}')} \right\rangle_{\mathcal{Q}} . \tag{2.29}$$

As a simple example of this type of expansion, an arbitrary projected coherent state $|\tilde{\alpha}\rangle$can be expanded using a CPS basis $\left\|\boldsymbol{\alpha}^{(\boldsymbol{q}')}\right\rangle_{\mathcal{Q}}$ with a different phase or radius. For this mapping of $\tilde{\alpha} \to \alpha^{(q)}$, on defining $z_q = \tilde{\alpha}/\alpha^{(q)}$, the expansion coefficient in the single-mode case has a rational function expression:

$$\psi_q(\tilde{\alpha}) = \frac{1}{d}\sum_{n=0}^{n_m} z_q^n = \frac{1}{d}\left[\frac{1-z_q^d}{1-z_q}\right] . \tag{2.30}$$

Alternatively, using normalized states with $\Psi_{\boldsymbol{q}} = g_{\mathcal{Q}}\psi_{\boldsymbol{q}}$so that$|\psi\rangle = \sum_{\boldsymbol{q}} \Psi_{\boldsymbol{q}} \left|\boldsymbol{\alpha}^{(\boldsymbol{q})}\right\rangle_{\mathcal{Q}}$, one would obtain:

$$\Psi_{\boldsymbol{q}}(\tilde{\alpha}) = \frac{g_{\mathcal{Q}}(\alpha)}{g_{\mathcal{Q}}(\tilde{\alpha})\, d}\left[\frac{1-z_q^d}{1-z_q}\right] . \tag{2.31}$$

III. PROJECTED STATE IDENTITIES

To use phase-space distributions in a calculation, one needs operator identities. These are employed to compute observables and calculate dynamical equations of motion. Here identities are obtained for operators acting on projected coherent states. For a projector $\hat{\mathcal{P}}$, there are invariant operators which satisfy $\hat{O}_I = \mathcal{P}\hat{O}_I\mathcal{P}$. Such operators have straightforward identities, and there are identities available in more general cases as well.

A. General projected identities

Many operators acting on coherent states correspond to simple differential forms. These differential identities are expressed as

$$\hat{O}\left\|\boldsymbol{\alpha}\right\rangle = \mathcal{D}(\boldsymbol{\alpha})\left\|\boldsymbol{\alpha}\right\rangle \tag{3.1}$$

where $\mathcal{D}(\boldsymbol{\alpha})$ is a differential operator of form $\mathcal{D}(\boldsymbol{\alpha}) = \sum_n D^{(n)}(\boldsymbol{\alpha})\,\partial_{i_1}\ldots\partial_{i_n}$, with the notation that:

$$\partial_i \equiv \frac{\partial}{\partial\alpha_i} . \tag{3.2}$$

In the projected case, there are differential identities available. If $\hat{O}_{\mathcal{P}}$ is a projected operator, one may define in analogy to (3.1) that:

$$\hat{O}_{\mathcal{P}}\left\|\boldsymbol{\alpha}\right\rangle_{\mathcal{P}} = \mathcal{D}_{\mathcal{P}}(\boldsymbol{\alpha})\left\|\boldsymbol{\alpha}\right\rangle_{\mathcal{P}} . \tag{3.3}$$

Detailed examples of these are given below; where they exist, they are very similar to those for the standard coherent states.

If the operator $\hat{O}$ is invariant, then $\mathcal{P}$ commutes both with $\hat{O}$ and with any differential operator $\mathcal{D}(\boldsymbol{\alpha})$, so that there is always one differential identity available that matches the non-projected case:

$$\hat{O}\left\|\boldsymbol{\alpha}\right\rangle_{\mathcal{P}} = \mathcal{D}(\boldsymbol{\alpha})\left\|\boldsymbol{\alpha}\right\rangle_{\mathcal{P}} . \tag{3.4}$$

For projections onto normalized coherent states, the invariant operator identities depend on the projection, because of the changed normalization factor. On rearranging the ordering of differential terms, this becomes:

$$\hat{O}\left|\boldsymbol{\alpha}\right\rangle_{\mathcal{P}} = \left[\mathcal{D} + a_{\mathcal{P}}\right]\left|\boldsymbol{\alpha}\right\rangle_{\mathcal{P}} . \tag{3.5}$$

where the c-number term $a_{\mathcal{P}}^{(\psi)}$ for state identities is obtained using a differential commutator:

$$a_{\mathcal{P}} = g_{\mathcal{P}}^{-1}\left[\mathcal{D}, g_{\mathcal{P}}\right] . \tag{3.6}$$

The differential commutator is defined in the usual way as $[\mathcal{D}, g(\boldsymbol{\alpha})] \equiv [\mathcal{D}g(\boldsymbol{\alpha}) - g(\boldsymbol{\alpha})\,\mathcal{D}]$, with differential operators acting on all functions to the right.

B. Number-conserving operator identities

To illustrate this, consider total number conserving operators acting on total number-projected coherent states. Similar identities hold as for the usual coherent states, since these operators are invariant.

For example, for the number operator $\hat{n} = \hat{a}^\dagger \hat{a}$ acting an unprojected coherent state, $\hat{n} \left\| \alpha \right\rangle = \alpha \partial_\alpha \left\| \alpha \right\rangle$. As expected from (3.4), for an invariant operator this identity is the same in the number-projected case:

$$\hat{n} \left\| \alpha \right\rangle_{\mathcal{N}} = \alpha \partial_\alpha \left\| \alpha \right\rangle_{\mathcal{N}} . \tag{3.7}$$

However, there is a change for *normalized* coherent states. Including normalization, the original non-projected identity is

$$\hat{n} \left| \alpha \right\rangle = \left[\alpha \partial_\alpha + \frac{1}{2} \left| \alpha \right|^2 \right] \left\| \alpha \right\rangle , \tag{3.8}$$

and on applying Eq (3.6) to the multi-mode case, one obtains the general result:

$$\hat{n}_{ij} \left| \boldsymbol{\alpha} \right\rangle_{\mathcal{N}} = \alpha_j \left[\partial_{\alpha_i} + \partial_{\alpha_i} \ln g_{\mathcal{N}} \right] \left| \boldsymbol{\alpha} \right\rangle_{\mathcal{N}} . \tag{3.9}$$

This is generally different to the identity of (3.8), since the normalization $g_{\mathcal{N}}$ depends on the projection.

C. Differential qudit identities

For qudit operator identities, the single mode number identities are invariant, so that if $\hat{n} = \hat{a}^\dagger \hat{a}$,

$$\hat{n} \left\| \alpha \right\rangle_{\mathcal{Q}} = \alpha \partial_\alpha \left\| \alpha \right\rangle_{\mathcal{Q}} , \tag{3.10}$$

and for a normalized qudit coherent state projection,

$$\hat{n} \left| \alpha \right\rangle_{Q} = \alpha \left[\partial_\alpha + \partial_\alpha \ln g_{\mathcal{Q}} \right] \left| \alpha \right\rangle_{Q} . \tag{3.11}$$

In the CPS case, the resulting normalized identities are similar to the usual coherent state identities, except for an additional correction term that vanishes for $n_0 \ll \left| \alpha \right|^2 \ll n_m$, since:

$$\partial_\alpha \ln g_{\mathcal{Q}} = \frac{\alpha^*}{2} \left[1 + \left(g^2_{n_0 - 1} - g^2_{n_m} \right) g_Q^{-2} \right] . \tag{3.12}$$

For annihilation or creation operators, which are non-invariant, one can still define projected operator identities following (3.3) . In a single-mode CPS, the action of the creation operator is:

$$\hat{a}^\dagger \left\| \alpha \right\rangle_{\mathcal{Q}} = \sum_{n=n_0}^{n_m} \frac{(n+1)\, \alpha^n}{\sqrt{(n+1)!}} \left| n+1 \right\rangle , \tag{3.13}$$

which leads to the differential identity:

$$\hat{a}^\dagger \left\| \alpha \right\rangle_{\mathcal{Q}} = \partial_\alpha \left[\left\| \alpha \right\rangle_{\mathcal{Q}} + \left| \alpha \right\rangle_{n_m + 1} - \left| \alpha \right\rangle_{n_0} \right] . \tag{3.14}$$

Therefore, on projection, one obtains a simple closed identity in the special case of $n_0 = 0$:

$$\hat{a}^\dagger_{\mathcal{Q}} \left\| \alpha \right\rangle_{\mathcal{Q}} = \partial_\alpha \left\| \alpha \right\rangle_{\mathcal{Q}} . \tag{3.15}$$

For the annihilation operator, the corresponding result is no longer simply expressed in terms of the original projected basis, since

$$\hat{a} \left\| \alpha \right\rangle_{\mathcal{Q}} = \alpha \left[\left\| \alpha \right\rangle_{\mathcal{Q}} + \left| \alpha \right\rangle_{n_0 - 1} - \left| \alpha \right\rangle_{n_m} \right] . \tag{3.16}$$

On projecting the operator, one obtains a closed identity which is asymptotically valid when the tails of the distribution g_n are negligible, so that

$$\hat{a}_{\mathcal{Q}} \left\| \alpha \right\rangle_{\mathcal{Q}} \cong \alpha \left\| \alpha \right\rangle_{\mathcal{Q}} . \tag{3.17}$$

If $n_0 = 0$, the lower limit correction vanishes. The high-n term becomes negligible exponentially fast as n_m is increased due to the Gaussian cut-off at large n_m. Another route is to use a small coherent radius, $r = \left| \alpha \right| \ll 1$, as the starting point of a CPS mapping, which can also strongly suppress the high-n residual term.

D. CPS matrix identities

For the CPS case, there are general matrix identities with the form

$$\hat{O}_{\mathcal{Q}} \left| \boldsymbol{\alpha}^{(\boldsymbol{q})} \right\rangle_{\mathcal{Q}} = \sum_{\boldsymbol{q}'} \mathcal{O}_{\boldsymbol{q}', \boldsymbol{q}} \left(\boldsymbol{\alpha} \right) \left| \boldsymbol{\alpha}^{(\boldsymbol{q}')} \right\rangle_{\mathcal{Q}} . \tag{3.18}$$

Utilizing the identity expansion (2.16), and introducing the matrix $O_{n'n}(\alpha) = g_{n'}^{-2} \left\langle \alpha \right\|_{n'} \hat{O} \left\| \alpha \right\rangle_n$, in the single-mode case this becomes:

$$\hat{O}_{\mathcal{Q}} \left| \alpha^{(q)} \right\rangle_{\mathcal{Q}} = g_{\mathcal{Q}}^{-1} \sum_{n,n'=0}^{d-1} e^{iqn\phi} O_{n'n}(\alpha) \left\| \alpha \right\rangle_{n'} . \tag{3.19}$$

Therefore, on inverting the mapping using the discrete Fourier transform theorem,

$$\hat{O}_{\mathcal{Q}} \left| \alpha^{(q)} \right\rangle_{\mathcal{Q}} = \sum_{q'=0}^{d-1} \mathcal{O}_{q'q} \left(\alpha \right) \left| \alpha^{(q')} \right\rangle_{\mathcal{Q}} . \tag{3.20}$$

where the matrix $\mathcal{O}_{q'q} \left(\alpha \right)$ is:

$$\mathcal{O}_{q'q} \left(\alpha \right) = \frac{1}{d} \sum_{n,n'=0}^{d-1} O_{n'n} \left(\alpha \right) e^{i(qn - q'n')\phi} . \tag{3.21}$$

One can therefore evaluate any pure state expectation value as:

$$\left\langle \hat{O} \right\rangle = \sum_{\boldsymbol{q}_i} \Psi^*_{\boldsymbol{q}_1} M_{\boldsymbol{q}_1 \boldsymbol{q}_2} \mathcal{O}_{\boldsymbol{q}_2 \boldsymbol{q}_3} \Psi_{\boldsymbol{q}_3} = \boldsymbol{\Psi}^\dagger \boldsymbol{M} \boldsymbol{\mathcal{O}} \boldsymbol{\Psi} . \tag{3.22}$$

where the inner-product matrix $M_{\boldsymbol{q}_1 \boldsymbol{q}_2} = \left\langle \boldsymbol{\alpha}^{(\boldsymbol{q}_1)} \right| \left. \boldsymbol{\alpha}^{(\boldsymbol{q}_2)} \right\rangle$ takes account of the non-orthogonality of the CPS basis. The choice of matrix or differential identity that is used depends on the requirements of a particular calculation. Differential identities are most useful for linear evolution, while matrix identities have more general applicability.

E. Hamiltonian evolution with CPS identities

As well as the differential results given above, the discrete identities for coherent phase states can be used to calculate the time evolution of a projection invariant state $|\psi(t)\rangle$. Firstly, the state is expanded in terms of the non-orthogonal CPS states, in the form

$$|\psi(t)\rangle = \sum_{q=0}^{d-1} \Psi_q(t) \left|\alpha^{(q)}\right\rangle_{\mathcal{Q}} . \tag{3.23}$$

Using a CPS mapping of $\hat{H}/\hbar \to \boldsymbol{\mathcal{H}}$, the Hamiltonian evolution of the expansions is given by:

$$i\frac{\partial}{\partial t}|\psi(t)\rangle = \sum_{q=0}^{d-1} \mathcal{H}_{q'q}\Psi_q(t) \left|\alpha^{(q)}\right\rangle_{\mathcal{Q}} . \tag{3.24}$$

To obtain the identities, for $\mathcal{H}$, the zero-based CPS case will be used here, with $n_0 = 0$.

The CPS matrices can be evaluated in common cases, by setting $z = \exp(i(q'-q)\phi)$, as follows:

$$\begin{aligned} \hat{a} \to \mathcal{O}^{[a]}_{q'q}(\alpha) &= \alpha^{(q)}\left[\delta_{qq'} - 1/d\right] \\ \hat{n}^k \to \mathcal{O}^{[k]}_{q'q} &= \frac{1}{d}\sum_{n=0}^{d-1} n^k z^n \\ \hat{a}^\dagger \to \mathcal{O}^{[a^\dagger]}_{q'q}(\alpha) &= \frac{1}{\alpha^{(q)}}\mathcal{O}^{[1]}_{q'q}. \end{aligned} \tag{3.25}$$

The projected identities are all matrix operations acting on the coherent phase states, which do not depend on the amplitude α for invariant operators. The identities for $\hat{n}^k$ involve sums over z that are well-known :

$$\begin{aligned} \mathcal{O}^{[1]}_{q'q} &= \frac{z - z^d\left[d - z(d-1)\right]}{d(1-z)^2} \\ &= (d-1)/2 \qquad (q = q') \\ \mathcal{O}^{[2]}_{q'q} &= \frac{z + z^2 - z^d\left[d - z(d-1)\right]^2 - z^{d+1}}{d(1-z)^3} \\ &= (d-1)(2d-1)/6 \qquad (q = q') . \end{aligned} \tag{3.26}$$

The nonlinear matrices grow with the cut-off d, although the matrix corresponding to $\hat{n}^2 - n_m\hat{n}$ has no terms except diagonals that grow with d :

$$\begin{aligned} O^{(2)}_{q'q} - n_m O^{(1)}_{q'q} &= z\frac{z^d(d-2) - d(z^{d-1} - z + 1) + 2}{(1-z)^3} \\ &= (d-1)(2-d)/6 \qquad (q = q') . \end{aligned} \tag{3.27}$$

After applying these identities, the time evolution of the vector of expansion coefficients $\boldsymbol{\Psi}$ is given by a unitary matrix $\boldsymbol{\mathcal{U}}(t) = \exp(-i\boldsymbol{\mathcal{H}}t)$:

$$\boldsymbol{\Psi}(t) = \boldsymbol{\mathcal{U}}(t)\boldsymbol{\Psi}(0). \tag{3.28}$$

This is a finite matrix equation, and directly uses the discrete Fourier transform identity (2.20).

Due to the linearity of quantum mechanics, the unitary evolution matrix $\boldsymbol{\mathcal{U}}(t)$ is independent of the initial state. This means that once $\boldsymbol{\mathcal{U}}(t)$ is known, the time evolution of any state within the projected manifold is immediately obtainable.

F. Hybrid pure-state evolution

From Eq (3.26), there is an unexpected invariance for Hamiltonians of form $\hat{n}^k$, which only depend on the particle number. In these cases, $\boldsymbol{\mathcal{U}}(t)$ is independent of the amplitude α. This can be used to obtain a novel type of factorization of the dynamical evolution. Consider a Hamiltonian with both a possibly time-dependent linear term $\hat{H}^{(0)}(t) = \hbar\omega_{ij}(t)\hat{a}_i^\dagger\hat{a}_j$ and a nonlinear term $\hat{H}^{(n)}$ which only has polynomial terms in $\hat{n}^k$, so that:

$$\hat{H} = \hat{H}^{(0)}(t) + \hat{H}^{(n)} . \tag{3.29}$$

One way to treat such problems is to use the interaction picture of quantum mechanics, in which operators evolve according to one part of the Hamiltonian and wavefunctions according to another. A variant of this approach is possible with projected coherent states. With this hybrid evolution approach, the base coherent state amplitude α evolves according to linear differential identities, while the phase indices q evolve according to nonlinear discrete identities which are independent of α.

In greater detail, one expands using both the discrete indices and the base amplitude, so that using Einstein summation over repeated $\boldsymbol{q}$ indices:

$$|\psi(t)\rangle = \int \Psi_{\boldsymbol{q}}(\boldsymbol{\alpha}, t)\left|\boldsymbol{\alpha}^{(\boldsymbol{q})}\right\rangle_{\mathcal{Q}} d\boldsymbol{\alpha} . \tag{3.30}$$

Under time-evolution,

$$i\hbar\frac{\partial}{\partial t}|\psi(t)\rangle = \int \Psi_{\boldsymbol{q}}(\boldsymbol{\alpha}, t)\hat{H}\left|\boldsymbol{\alpha}^{(\boldsymbol{q})}\right\rangle_{\mathcal{Q}} d\boldsymbol{\alpha} . \tag{3.31}$$

Next, one uses identities so that $\hat{H}^{(0)}(t)/\hbar \to \mathcal{D}(\boldsymbol{\alpha}, t)$, $\hat{H}^{(n)}/\hbar \to \boldsymbol{\mathcal{H}}^{(n)}$. Provided partial integration is possible, leading to a partially integrated operator $\mathcal{D}'(\boldsymbol{\alpha}, t)$, the resulting time-evolution equation is:

$$\dot{\Psi}_{\boldsymbol{q}}(\boldsymbol{\alpha}, t) = -i\left[\mathcal{D}'(\boldsymbol{\alpha}, t) + \mathcal{H}^{(n)}_{\boldsymbol{qq'}}\right]\Psi_{\boldsymbol{q}}(\boldsymbol{\alpha}, t) . \tag{3.32}$$

If $\mathcal{H}^{(n)}_{\boldsymbol{qq'}}$ is independent of $\boldsymbol{\alpha}$, which is true with number-conserving nonlinear Hamiltonians, one may introduce an integrating factor $\boldsymbol{\mathcal{U}}^{(n)}(t) = \exp\left(-i\boldsymbol{\mathcal{H}}^{(n)}t\right)$ such that $\Psi_{\boldsymbol{q}}(t) = \boldsymbol{\mathcal{U}}^{(n)}(t)\Psi^{(n)}_{\boldsymbol{q}}(t)$, $\tilde{\mathcal{D}}'(\boldsymbol{\alpha}, t) = \boldsymbol{\mathcal{U}}^{(n)\dagger}(t)\mathcal{D}'(\boldsymbol{\alpha}, t)\boldsymbol{\mathcal{U}}^{(n)}(t)$. The resulting differential equation is then:

$$\dot{\Psi}^{(n)}_{\boldsymbol{q}}(\boldsymbol{\alpha}, t) = \tilde{\mathcal{D}}'(\boldsymbol{\alpha}, t)\,\Psi^{(n)}_{\boldsymbol{q}}(\boldsymbol{\alpha}, t) . \tag{3.33}$$

This has the unusual feature that it is the nonlinear term rather than the linear term that is removed in the interaction picture. For single mode Hamiltonians the situation is even simpler, since $\tilde{\mathcal{D}}'(\boldsymbol{\alpha},t) = \mathcal{D}'(\boldsymbol{\alpha},t) = i\omega(t)\partial_\alpha\alpha$. In this case the time evolution factorizes completely, such that α can be treated as a characteristic trajectory obeying $\dot{\alpha}(t) = -i\omega\alpha(t)$. This causes a rotation in the reference amplitude α, while the nonlinear terms independently modify the discrete indices q .

IV. PROJECTED P-REPRESENTATIONS

The generalized P-representation maps a quantum Hilbert space to a phase-space of double the classical dimensionality [5, 44]. It provides a natural way to represent mixed states rather than just pure states, and is especially useful in open and exponentially complex systems. Yet if just part of a Hilbert space is physically important, due to a symmetry or other reasons, it is more efficient to only map the projected part of the space.

For such projected measurements, it is irrelevant whether one projects the density matrix, the measured operator, or both. Given a density matrix $\hat{\rho}$ or an operator $\hat{O}$, their projected versions are $\hat{\rho}_{\mathcal{P}}$ and $\hat{O}_{\mathcal{P}}$ respectively. Projections of the density matrix allow the treatment of all possible projected measurements in a unified way. For projected phase-space representations, suppose that the density matrix $\hat{\rho}$ is invariant under the projection, i.e.,

$$\hat{\rho} = \hat{\rho}_{\mathcal{P}} = \mathcal{P}\hat{\rho}\mathcal{P}\,. \tag{4.1}$$

This section will develop efficient mappings onto a phase-space for density matrices of this type, that occupy only a fractional part of the Hilbert space. The projection types are as in the earlier sections. Two different types of identity, for normalized or un-normalized representations, are treated.

A. Generalized P-representations

It is useful to first review the P-representation phase-space method. This was originally proposed in a diagonal form [6, 7], where it was crucial to the development of coherence and laser theory. Since this gave singular results for nonclassical states, the generalized P-representation was introduced for all quantum states [10], with the form:

$$\hat{\rho} = \int P\left(\overrightarrow{\boldsymbol{\alpha}}\right)\hat{\Lambda}\left(\overrightarrow{\boldsymbol{\alpha}}\right)d\mu\,. \tag{4.2}$$

Here $\overrightarrow{\boldsymbol{\alpha}} \equiv (\boldsymbol{\alpha},\boldsymbol{\beta})$ denotes a double-dimensional coherent amplitude, and the operator basis used in the expansion is:

$$\hat{\Lambda}\left(\overrightarrow{\boldsymbol{\alpha}}\right) \equiv e^{-\boldsymbol{\alpha}\cdot\boldsymbol{\beta}}\left\|\boldsymbol{\alpha}\right\rangle\left\langle\boldsymbol{\beta}^*\right\| = G^{-1}\left(\overrightarrow{\boldsymbol{\alpha}}\right)\hat{\lambda}\left(\overrightarrow{\boldsymbol{\alpha}}\right). \tag{4.3}$$

The normalizing factor is $G\left(\overrightarrow{\boldsymbol{\alpha}}\right) = \exp\left[\boldsymbol{\alpha}\cdot\boldsymbol{\beta}\right]$, which reduces to $g^2(\boldsymbol{\alpha})$ as in (2.5), in the diagonal limit of $\boldsymbol{\alpha} = \boldsymbol{\beta}^*$. In positive P-representations, the integration measure $d\mu$ is a volume measure, $d\mu = d^{2M}\boldsymbol{\alpha}d^{2M}\boldsymbol{\beta}$, which has double the classical dimension. The measure can also be a contour integral, so that $d\mu = d\boldsymbol{\alpha}d\boldsymbol{\beta}$, and the distribution function $P\left(\overrightarrow{\boldsymbol{\alpha}}\right)$ is complex-valued. There are several existence theorems for the full Hilbert space [45, 46].

- A positive, normally ordered standard positive P-distribution exists for all quantum states. While this construction is always available, it is often not the most compact form.
- A complex P-representation, requiring a contour integral around the origin, exists for all states with a bounded support in number or coherent states. This approach can give a very compact distribution. It is a special case of more general gauge, or complex weighted methods, that are useful in simulating quantum dynamics [47].

In both cases, the representation gives observable normally-ordered correlation functions that are classical-like moments of the distribution.

B. Projected P-representations

The projected P-representation has a similar construction to the generalized P-representation, except that it makes use of a projected operator basis, so that:

$$\hat{\rho} = \int p\left(\overrightarrow{\boldsymbol{\alpha}}\right)\hat{\lambda}_{\mathcal{P}}\left(\overrightarrow{\boldsymbol{\alpha}}\right)d\mu\,. \tag{4.4}$$

$$= \int P\left(\overrightarrow{\boldsymbol{\alpha}}\right)\hat{\Lambda}_{\mathcal{P}}\left(\overrightarrow{\boldsymbol{\alpha}}\right)d\mu\,. \tag{4.5}$$

Here, the unnormalized projected basis $\hat{\lambda}_{\mathcal{P}}$ is:

$$\hat{\lambda}_{\mathcal{P}}\left(\overrightarrow{\boldsymbol{\alpha}}\right) \equiv \left\|\boldsymbol{\alpha}\right\rangle_P\left\langle\boldsymbol{\beta}^*\right\|_P\,. \tag{4.6}$$

and the projected basis $\hat{\Lambda}_P$ normalized so that $Tr\left(\hat{\Lambda}_P\right) = 1$ is

$$\hat{\Lambda}_{\mathcal{P}}\left(\overrightarrow{\boldsymbol{\alpha}}\right) \equiv G_{\mathcal{P}}^{-1}\left(\overrightarrow{\boldsymbol{\alpha}}\right)\hat{\lambda}_{\mathcal{P}}\left(\overrightarrow{\boldsymbol{\alpha}}\right), \tag{4.7}$$

so that $p\left(\overrightarrow{\boldsymbol{\alpha}}\right) = G_{\mathcal{P}}^{-1}\left(\overrightarrow{\boldsymbol{\alpha}}\right)P\left(\overrightarrow{\boldsymbol{\alpha}}\right)$. The normalization factor, $G_P\left(\overrightarrow{\boldsymbol{\alpha}}\right) \equiv \left\langle\boldsymbol{\beta}^*\right\|\boldsymbol{\alpha}\rangle_{\mathcal{P}}$, is the inner product of two unnormalized projected coherent states, so that for number projections:

$$G_{\mathcal{N}}\left(\overrightarrow{\boldsymbol{\alpha}}\right) = \sum_{\boldsymbol{n}\in S}\prod_i \frac{\left(\beta_i\alpha_i\right)^{n_i}}{n_i!}\,. \tag{4.8}$$

The projected P-distribution is generally different to the standard P-distribution, even for an identical density

matrix. The reason for this is that the operator basis has a changed normalization. Unless one takes the limit of $G_{\mathcal{P}}\left(\overrightarrow{\boldsymbol{\alpha}}\right) \to 1$, the normalized projected basis is not just a projection of the normalized basis, i.e., in general

$$\hat{\Lambda}_{\mathcal{P}}\left(\overrightarrow{\boldsymbol{\alpha}}\right) \neq \mathcal{P}\hat{\Lambda}\left(\overrightarrow{\boldsymbol{\alpha}}\right)\mathcal{P}\,. \tag{4.9}$$

This is because the full operator basis extends over the entire Hilbert space, so it has a different normalization. For a projection invariant density matrix, the unprojected distribution has to ensure that the expansion in coherent states has no contribution from the additional part of the Hilbert space. This is not required of the projected distribution. One can obtain a projected distribution from an unprojected one, by first projecting then renormalizing it.

The expansions are identical in the limit $|\boldsymbol{\alpha}| \to 0$, $|\boldsymbol{\beta}| \to 0$, where $G_{\mathcal{P}}\left(\overrightarrow{\boldsymbol{\alpha}}\right) \to 1$. The un-normalized projected operator basis is similar to the unprojected case, since

$$\hat{\lambda}_{\mathcal{P}}\left(\overrightarrow{\boldsymbol{\alpha}}\right) = \mathcal{P}\hat{\lambda}\left(\overrightarrow{\boldsymbol{\alpha}}\right)\mathcal{P}\,. \tag{4.10}$$

However, this is not the case for the normalized basis, due to the additional normalizing factor.

C. Existence of number-projected P-distributions

A similar method can be to obtain existence theorems for the number-projected case as for the complex P-representation [5]. Recalling the definition of $\|\boldsymbol{\alpha}\rangle_{\boldsymbol{n}}$, and using Cauchy's theorem, a contour integral simply projects out the appropriate number state. On substitution into the general definition of the projected phase-space representation, an un-normalized P-representation is obtained where:

$$p\left(\overrightarrow{\boldsymbol{\alpha}}\right) = \sum_{\boldsymbol{nm}\in S} \frac{\rho_{\mathbf{mn}}}{\left(2\pi i\right)^{2M}} \int d\mu \prod_j \frac{\sqrt{n_j! m_j!}}{\beta_j^{n_j+1}\alpha_j^{m_j+1}}\,. \tag{4.11}$$

This contour integral method can be used to obtain existence theorems for any finite state case, regardless of which type of number projection is used. This gives a continuous rather than a discrete distribution, which is complex-valued. It is applicable to both normalized and un-normalized cases, since one can always obtain a normalized distribution through the relationship that $P = pG_{\mathcal{P}}$.

There appears to be no corresponding exact construction for projected positive P-distributions, except in special cases. This is not a significant issue: one can still calculate observables with complex weights.

D. CPS P-representations

In the case of coherent phase states, from (II E), one can define the measure as a discrete summation over a set $\tilde{S}$ of d^{2M} coherent amplitudes that is complementary to the projected set S. This is similar to a contour integral, except that the distribution is a sum over delta-functions in a circle, not a continuous integral. Here, one defines the CPS amplitudes similarly to a wave-function expansion, so that:

$$\begin{aligned}\alpha^{(q)} &\equiv \alpha \exp\left(iq\phi\right),\\ \beta^{(q)} &\equiv \beta \exp\left(-iq\phi\right), \quad q = 0, \ldots d-1.\end{aligned} \tag{4.12}$$

This is identical to defining $P_{\mathcal{Q}}\left(\overrightarrow{\boldsymbol{\alpha}}\right)$ as a delta-function at each discrete point in phase-space. In the CPS case, one can introduce a set of basis operators $\hat{\lambda}_{\overrightarrow{\boldsymbol{q}}}\left(\overrightarrow{\boldsymbol{\alpha}}\right) \equiv \hat{\lambda}_{\mathcal{Q}}\left(\boldsymbol{\alpha}^{(\boldsymbol{q})}, \boldsymbol{\beta}^{(\boldsymbol{q}')}\right)$, where $\overrightarrow{\boldsymbol{q}} \equiv (\boldsymbol{q}, \boldsymbol{q}')$. The normalization factor is $G_{\overrightarrow{\boldsymbol{q}}}\left(\overrightarrow{\boldsymbol{\alpha}}\right) = G_{\mathcal{Q}}\left(\boldsymbol{\alpha}^{(\boldsymbol{q})}, \boldsymbol{\beta}^{(\boldsymbol{q}')}\right)$ and the corresponding normalized basis is defined as:

$$\begin{aligned}\hat{\Lambda}_{\overrightarrow{\boldsymbol{q}}}\left(\overrightarrow{\boldsymbol{\alpha}}\right) &\equiv \hat{\Lambda}_{\mathcal{Q}}\left(\boldsymbol{\alpha}^{(\boldsymbol{q})}, \boldsymbol{\beta}^{(\boldsymbol{q}')}\right).\\ &= \hat{\lambda}_{\overrightarrow{\boldsymbol{q}}}\left(\overrightarrow{\boldsymbol{\alpha}}\right)/G_{\overrightarrow{\boldsymbol{q}}}\left(\overrightarrow{\boldsymbol{\alpha}}\right).\end{aligned}$$

The representation is then written as:

$$\begin{aligned}\hat{\rho} &= \sum_{\overrightarrow{\boldsymbol{q}}} p_{\overrightarrow{\boldsymbol{q}}}\left(\overrightarrow{\boldsymbol{\alpha}}\right)\hat{\lambda}_{\overrightarrow{\boldsymbol{q}}}\left(\overrightarrow{\boldsymbol{\alpha}}\right)\\ &= \sum_{\overrightarrow{\boldsymbol{q}}} P_{\overrightarrow{\boldsymbol{q}}}\left(\overrightarrow{\boldsymbol{\alpha}}\right)\hat{\Lambda}_{\overrightarrow{\boldsymbol{q}}}\left(\overrightarrow{\boldsymbol{\alpha}}\right),\end{aligned} \tag{4.13}$$

The single-mode normalization coefficient is given explicitly by:

$$G_{\mathcal{Q}}\left(\alpha, \beta\right) = \sum_{n=n_0}^{n_m} \frac{\left(\beta\alpha\right)^n}{n!}\,. \tag{4.14}$$

CPS P-representations for projected density matrices using coherent phase states can be found following the methods given in Section (II D). As described in Section (II E), this method can be utilized if the set of occupation numbers for mode j has the form $n_j = n_0, \ldots n_m$, where $n_m = d + n_0 - 1$. An example is for $n_0 = 0$, so that the first state is the vacuum state. With this expansion, a unique CPS P-function $p_{\mathbf{q},\mathbf{q}'}$ always exists given $\rho_{\mathbf{mn}} = \langle \boldsymbol{m}| \widehat{\rho}_{\mathcal{Q}} |\boldsymbol{n}\rangle$, where:

$$p_{\mathbf{q},\mathbf{q}'} = \sum_{\boldsymbol{n},\boldsymbol{m}\in S} \rho_{\mathbf{mn}} \prod_j \frac{\sqrt{n_j! m_j!}}{d^2\left(\alpha_j^{(q_j)}\right)^{m_j}\left(\beta_j^{(q'_j)}\right)^{n_j}}\,. \tag{4.15}$$

Consequently, a normalized $P_{\mathbf{q},\mathbf{q}'} = p_{\mathbf{q},\mathbf{q}'}G_{\mathbf{q},\mathbf{q}'}$. This can be verified as a solution by inserting this distribution into the expansion of the density matrix, noting that, from the properties of the discrete Fourier transform,

$$\frac{1}{d^M}\sum_{\mathbf{k}} e^{i\boldsymbol{q}\cdot(\boldsymbol{n}-\boldsymbol{m})} = \delta_{\boldsymbol{n}-\boldsymbol{m}}\,. \tag{4.16}$$

This approach is independent of the base amplitudes $\alpha$and β. A second method of expansion is that if one

representation is known that uses a coherent projector on a different basis with $\hat{\lambda}_Q\left(\tilde{\boldsymbol{\alpha}},\tilde{\boldsymbol{\beta}}\right)$, one can map $\tilde{\alpha},\tilde{\beta}\rightarrow\alpha^{(q)},\beta^{(q)}$ using Eq (2.30), so that:

$$\hat{\lambda}_Q\left(\tilde{\boldsymbol{\alpha}},\tilde{\boldsymbol{\beta}}\right)=\sum_{\overrightarrow{q}}\tilde{p}_{\overrightarrow{q}}\hat{\lambda}_{\overrightarrow{q}}\,. \tag{4.17}$$

This allows the transformation of any projected P-function into another one that uses another basis set, even with a different radius. With the usual, unprojected complex P-representation, this type of transformation is known when the contour radius is increased, allowing the use of Cauchy's theorem [45]. In the projected case, any basis element $\hat{\lambda}_Q\left(\tilde{\boldsymbol{\alpha}},\tilde{\boldsymbol{\beta}}\right)$ can be re-expanded using a CPS basis $\hat{\lambda}_{\overrightarrow{\boldsymbol{q}}}$. The expansion coefficient is similar to the corresponding CPS expression in Eq (2.30). Defining $z_q=\tilde{\alpha}/\alpha^{(q)}$, $\zeta_q=\tilde{\beta}/\beta^{(q)}$, the coefficient is:

$$\tilde{p}_{\overrightarrow{q}}=\frac{1}{d^2}\left[\frac{1-z_q^d}{1-z_q}\right]\left[\frac{1-\zeta_{q'}^d}{1-\zeta_{q'}}\right]\,. \tag{4.18}$$

A consequence of this construction is that if necessary, one can take the small radius limit of $\alpha_j,\beta_j\equiv r\rightarrow 0$. In this limit, the normalizing factor is unity, i.e., $G\rightarrow 1$. This means that the projected distribution is identical to an unprojected complex P-distribution obtained as a sum of delta-functions for the same contour, even though the basis is changed. This feature is useful in calculations [18] for photonic networks.

E. Unnormalized operator identities

Applications of phase-space representations to quantum physics depend on the existence of many operator identities, which are closely related to the coherent state differential identities of Section (III). Operators acting on $\hat{\Lambda}$ that correspond to differential operators acting on P allow evaluation of mean expectation values for the quantum density matrix, as well dynamical evolution equations for the distribution. This first requires knowledge of a the operator identities.

In the non-projected case, one obtains:

$$\begin{aligned}\hat{a}\hat{\lambda}&=\alpha\hat{\lambda}\,.\\ \hat{a}^{\dagger}\hat{\lambda}&=\partial_{\alpha}\hat{\lambda}\\ \hat{n}\hat{\lambda}&=\alpha\partial_{\alpha}\hat{\lambda}\,.\end{aligned} \tag{4.19}$$

The consequence of this is that any normally ordered correlation function is easily evaluated, giving

$$\left\langle a_{m_1}^{\dagger}\ldots a_{m_n}\right\rangle=\int\beta_{m_1}\ldots\alpha_{m_n}P\left(\overrightarrow{\boldsymbol{\alpha}}\right)d\mu\,. \tag{4.20}$$

What are the corresponding operator identities in the projected case? For unnormalized P-representations, the identities have an identical structure to that of 3.3, so that for certain operators $\hat{O}$,

$$\begin{aligned}\hat{O}_{\mathcal{P}}\hat{\lambda}_{\mathcal{P}}&=\mathcal{D}_{\mathcal{P}}\left(\boldsymbol{\alpha}\right)\hat{\lambda}_{\mathcal{P}}\\ \hat{\lambda}_{\mathcal{P}}\hat{O}_{\mathcal{P}}^{\dagger}&=\mathcal{D}_{\mathcal{P}}\left(\boldsymbol{\beta}\right)\hat{\lambda}_{\mathcal{P}}\,.\end{aligned} \tag{4.21}$$

For invariant operators that commute with $\mathcal{P}$, the projection of an operator product $\hat{O}\hat{\lambda}$ or $\hat{\lambda}\hat{O}$ has a differential identity on $\hat{\lambda}_{\mathcal{P}}$, since:

$$\mathcal{P}\hat{O}\hat{\lambda}\mathcal{P}=\mathcal{P}\mathcal{D}\hat{\lambda}\mathcal{P}=\mathcal{D}\hat{\lambda}_{\mathcal{P}}. \tag{4.22}$$

Hence, given an operator $\hat{O}$ that commutes with the projector $\mathcal{P}$, the basis identities of 4.19 must follow in the projected case as well. Typical examples are identical to those given for projected coherent states, so for example,

$$\hat{n}\hat{\lambda}_{\mathcal{N}}=\alpha\partial_{\alpha}\hat{\lambda}_{\mathcal{N}}\,. \tag{4.23}$$

For the CPS case, the general matrix identities of (3.18) are directly applicable, giving the result that:

$$\begin{aligned}\hat{O}_{\mathcal{Q}}\hat{\lambda}_{\overrightarrow{\boldsymbol{q}}}&=\sum_{\boldsymbol{q}"}\mathcal{O}_{\boldsymbol{q}",\boldsymbol{q}}\left(\boldsymbol{\alpha}\right)\hat{\lambda}_{\boldsymbol{q}",\boldsymbol{q}'}\\ \hat{\lambda}_{\overrightarrow{\boldsymbol{q}}}\hat{O}_{\mathcal{Q}}^{\dagger}&=\sum_{\boldsymbol{q}'}\mathcal{O}_{\boldsymbol{q}",\boldsymbol{q}'}^{*},\left(\boldsymbol{\beta}^{*}\right)\hat{\lambda}_{\boldsymbol{q},\boldsymbol{q}"}\,.\end{aligned} \tag{4.24}$$

F. Normalized operator identities

The corresponding identities for the normalized basis operators are modified, since the normalizing terms are different after projection. Thus, one obtains:

$$\hat{O}\hat{\Lambda}_{\mathcal{P}}=G_{\mathcal{P}}\hat{O}\hat{\lambda}_{\mathcal{P}}=G_{\mathcal{P}}\mathcal{D}\hat{\lambda}_{\mathcal{P}} \tag{4.25}$$

On re-arranging the ordering of differential terms, this becomes:

$$\begin{aligned}\hat{O}\hat{\Lambda}_{\mathcal{P}}&=\left[\mathcal{D}\left(\boldsymbol{\alpha}\right)+\mathcal{A}\left(\overrightarrow{\boldsymbol{\alpha}}\right)\right]\hat{\Lambda}_{\mathcal{P}}\\ \hat{\Lambda}_{\mathcal{P}}\hat{O}^{\dagger}&=\left[\mathcal{D}\left(\boldsymbol{\beta}\right)+\mathcal{A}\left(\boldsymbol{\beta},\boldsymbol{\alpha}\right)\right]\hat{\Lambda}_{\mathcal{P}}\end{aligned} \tag{4.26}$$

where the c-number terms $\mathcal{A}$ for are given in terms of a differential commutator. These are similar to the coherent state identities, except that the normalizing factor is different:

$$\mathcal{A}=G_{\mathcal{P}}^{-1}\left[\mathcal{D},G_{\mathcal{P}}\right]\,. \tag{4.27}$$

It is also possible to obtain identities for more general operator products that occur in master equations. These are of the form $\hat{O}_1\hat{\rho}\hat{O}_2$, which are invariant provided that:

$$\mathcal{P}\hat{O}_1\hat{\rho}\hat{O}_2\mathcal{P}=\hat{O}_1\mathcal{P}\hat{\rho}\mathcal{P}\hat{O}_2 \tag{4.28}$$

However, the corresponding identities are best worked out on a case-by case basis.

Unlike the quantum state matrix identities, which do not depend on the normalization, the matrix operator

identities for the CPS basis change when normalized P-representations are considered. The reason for this is that the normalization factors are state-dependent. As a a result, the above matrix identities are modified, and become:

$$\hat{O}_{\mathcal{Q}}\hat{\Lambda}_{\overrightarrow{\boldsymbol{q}}} = G^{-1}_{\overrightarrow{\boldsymbol{q}}}\sum_{\boldsymbol{q}^{"}} G_{\boldsymbol{q}^{"},\boldsymbol{q}'}\mathcal{O}_{\boldsymbol{q}^{"},\boldsymbol{q}}\left(\boldsymbol{\alpha}\right)\hat{\Lambda}_{\boldsymbol{q}^{"},\boldsymbol{q}'}$$
$$\hat{\Lambda}_{\overrightarrow{\boldsymbol{q}}}\hat{O}^{\dagger}_{\mathcal{Q}} = G^{-1}_{\overrightarrow{\boldsymbol{q}}}\sum_{\boldsymbol{q}'} G_{\boldsymbol{q},\boldsymbol{q}^{"}}\mathcal{O}^{*}_{\boldsymbol{q}^{"},\boldsymbol{q}'},\left(\boldsymbol{\beta}^{*}\right)\hat{\lambda}_{\boldsymbol{q},\boldsymbol{q}^{"}}\,. \tag{4.29}$$

Example: the number operator As an example, for the single-mode number operator $\hat{n}_i = \hat{a}^{\dagger}_i\hat{a}_i$, one obtains the differential operator

$$\hat{n}_i\left\|\boldsymbol{\alpha}\right\rangle_{\mathcal{N}}\left\langle\boldsymbol{\beta}^{*}\right\|_{\mathcal{N}} = \alpha_i\partial_i\left\|\boldsymbol{\alpha}\right\rangle_{\mathcal{N}}\left\langle\boldsymbol{\beta}^{*}\right\|_{\mathcal{N}}\,. \tag{4.30}$$

Consequently, in the single mode case, with the normalization factor included:

$$\hat{n}\hat{\Lambda}_{\mathcal{N}} = \alpha\left[\partial_\alpha + \left(\partial_\alpha \ln G_{\mathcal{N}}\right)\right]\hat{\Lambda}_{\mathcal{N}} = \left[\mathcal{D}+\mathcal{A}\right]\hat{\Lambda}_{\mathcal{N}}\,. \tag{4.31}$$

Here the notation $\left(\partial_\alpha \ln G_{\mathcal{N}}\right) \equiv \mathcal{A}$ indicates that the derivative only acts on the term in the brackets. For an ensemble average, it follows that:

$$\left\langle\hat{n}\right\rangle = Tr\left(\int P_{\mathcal{N}}\left(\alpha,\beta\right)\left[\mathcal{D}+\mathcal{A}\right]\hat{\Lambda}_{\mathcal{N}}d\mu\right)\,. \tag{4.32}$$

On partial integration and introducing $\mathcal{D}' = \partial_\alpha\alpha$ as the re-ordered version of $\mathcal{D}$, after partial integration, together with the condition that $Tr\left(\hat{\Lambda}_{\mathcal{N}}\right) = 1$, one obtains:

$$\left\langle\hat{n}\right\rangle = \int\left[\mathcal{A}-\mathcal{D}'\right]P_{\mathcal{N}}\left(\alpha,\beta\right)d\mu\,. \tag{4.33}$$

Since the integral of a total derivative vanishes due to the boundary conditions, the final result is a simple moment over the distribution:

$$\left\langle\hat{n}\right\rangle = \int\mathcal{A}P_{\mathcal{N}}\left(\alpha,\beta\right)d\mu\,. \tag{4.34}$$

In the CPS case, $\mathcal{A} = \alpha\partial_\alpha \ln\sum_{n=n_0}^{n_m}\left(\beta\alpha\right)^n/n!$, which reduces to $\mathcal{A} = \alpha\beta$ at large cutoff, as one expects.

G. Time evolution

Just as with pure states, the evolution of a mixed state density matrix can be treated in three ways: using differential identities, discrete identities, or with a hybrid approach, combining linear differential terms and nonlinear discrete matrix evolution for CPS mappings. The hybrid approach is useful in some cases, since it removes the large sampling error that can happen if time-evolution is treated using stochastic equations derived purely from a Fokker-Planck equation.

Consider a Liouvillian that includes loss and decoherence, with both linear and nonlinear terms, so that:

$$\mathcal{L} = \mathcal{L}^{(0)} + \mathcal{L}^{(n)}\,, \tag{4.35}$$

where $\mathcal{L}^{(0)}$ describes the linear evolution and $\mathcal{L}^{(n)}$ the nonlinear part. Usually one must calculate time-evolution using a master equation when there is coupling to reservoirs and dissipation, so that:

$$\mathcal{L}\left[\hat{\rho}\right] = \frac{-i}{\hbar}\left[\hat{H},\hat{\rho}\right] + \sum_j \gamma_j(2A_j\hat{\rho}A_j^{\dagger} - A_j^{\dagger}A_j\hat{\rho} - \hat{\rho}A_j^{\dagger}A_j)\,,$$

where $\hat{H}$ is the system Hamiltonian, γ_j are a set of decay rates, and $\hat{A}_j$ are the corresponding operators that describe coupling to reservoirs that cause decoherence. In the differential approach, time-evolution is then obtained by transforming the operators acting on $\hat{\lambda}$ or $\hat{\Lambda}$ to differential operators, integrating by parts if this is possible, then solving the resulting equations.

In the hybrid evolution approach, the base coherent state amplitudes α,β evolve according to linear differential identities, while the phase indicesq,q' evolve according to nonlinear discrete identities. This has an advantage compared to the usual interaction picture, in that any type of linear evolution is easily treated in this fashion, including losses described by a master equation.

In greater detail, one expands using both the discrete indices and the base amplitude, so that using Einstein summation over repeated $\boldsymbol{q}$ indices:

$$\hat{\rho} = \int p_{\overrightarrow{\boldsymbol{q}}}\left(\overrightarrow{\boldsymbol{\alpha}}\right)\hat{\lambda}_{\overrightarrow{\boldsymbol{q}}}\left(\overrightarrow{\boldsymbol{\alpha}}\right)d\mu\,, \tag{4.36}$$

Under time-evolution,

$$\frac{\partial}{\partial t}\hat{\rho} = \int p_{\overrightarrow{\boldsymbol{q}}}\left(\overrightarrow{\boldsymbol{\alpha}}\right)\left\{\mathcal{L}^{(0)}\left[\hat{\lambda}_{\overrightarrow{\boldsymbol{q}}}\right] + \mathcal{L}^{(n)}\left[\hat{\lambda}_{\overrightarrow{\boldsymbol{q}}}\right]\right\}d\mu\,. \tag{4.37}$$

Next, suppose that one uses identities so that $\mathcal{L}^{(0)} \rightarrow \mathcal{D}\left(\overrightarrow{\boldsymbol{\alpha}}\right)$, $\hat{H}^{(n)} \rightarrow \boldsymbol{\mathcal{H}}^{(n)}$. Provided partial integration is possible with vanishing boundary terms, the resulting time-evolution equation is:

$$\dot{p}_{\overrightarrow{\boldsymbol{q}}}\left(\overrightarrow{\boldsymbol{\alpha}}\right) = \left[\mathcal{D}'\left(\overrightarrow{\boldsymbol{\alpha}}\right)\delta_{\overrightarrow{\boldsymbol{q}}\,\overrightarrow{\boldsymbol{q}}'} + \mathcal{L}^{(n)}_{\overrightarrow{\boldsymbol{q}}\,\overrightarrow{\boldsymbol{q}}'}\right]p_{\overrightarrow{\boldsymbol{q}}'}\left(\overrightarrow{\boldsymbol{\alpha}}\right)\,, \tag{4.38}$$

where the partially integrated operator $\mathcal{D}'\left(\overrightarrow{\boldsymbol{\alpha}}\right)$ reverses the order of differentiation and changes the sign of each differential term.

V. EXAMPLES

There are many ways to use these techniques, depending on the projections and symmetries involved. It is impossible to cover all the relevant applications in one paper. The details in each case are subtly different, and

this needs to be taken into account in individual problems. In this section, three simple illustrative examples are covered, based on recent experiments in atom optics and photonics. The examples use the CPS basis, but this is only one type of projection. Others are also useful, and can be treated with the same general approach.

A. Anharmonic oscillator coherent dynamics

To understand how to use these techniques, consider the dynamical evolution of a quantum anharmonic oscillator, which has both recurrences and macroscopic superpositions. This is highly nontrivial to treat using other phase-space methods [48, 49], owing to its nonclassical behavior. It is exactly soluble in the lossless single-mode case [46, 50], and revivals have been experimentally investigated [51]. As such, it is a useful test case, and the present techniques can be used to extend these results to include real-world decoherence effects.

The Hamiltonian in the single-mode case is:

$$\hat{H}/\hbar = \omega\hat{n} + \frac{1}{2}\kappa\hat{n}^2\,. \tag{5.1}$$

In the graphs below, the evolution of a projected coherent state $|\alpha\rangle_{\mathcal{Q}}$ is directly computed using a circular basis of CPS states with the same radius, $r = |\alpha_0|$. Time-evolution results are obtained by exponentiating the Hamiltonian matrix over a small interval Δt to give

$$\boldsymbol{\psi}(t+\Delta t) = \exp\left(-i\boldsymbol{\mathcal{H}}^A\Delta t\right)\boldsymbol{\psi}(t)\,, \tag{5.2}$$

where the Hamiltonian matrix $\boldsymbol{\mathcal{H}}^A$ is

$$\boldsymbol{\mathcal{H}}^A = \omega\boldsymbol{\mathcal{O}}^{[1]} + \frac{1}{2}\kappa\boldsymbol{\mathcal{O}}^{[2]}\,.$$

Apart from round-off errors, this is an exact procedure.

The analytical solution has an especially simple form for the average coherent amplitude with no projection,

$$\langle\hat{a}\rangle_\infty = \alpha\exp\left[|\alpha|^2\left(e^{-i\kappa t}-1\right) - i\left(\omega+\kappa/2\right)t\right] \tag{5.3}$$

The quantity plotted is the average coherent amplitude $\langle\hat{a}\rangle_d$ for $\alpha = 4$, with parameters $\chi = 1$ and $\omega = 0.5$ and a projection of $n < d$. For these parameters, an exact revival occurs at $t = 2n\pi$, for $n = 1, 2, \ldots$. Numerical results are shown in Fig (4), using a cutoff of at $d = 2\alpha^2 = 32$ and 500 time-steps.

A graph of the difference between the projected and analytic result is shown in Fig (5), showing that the maximum change in amplitude due to the number cut-off is 3×10^{-3}. This shows that these techniques can be readily applied to a model of nonlinear quantum dynamics.

The approach can be easily extended to larger cutoff values. Fig (6) shows the effect of changing both cutoff and using the hybrid picture, so that the linear evolution takes place using an interaction picture, in which

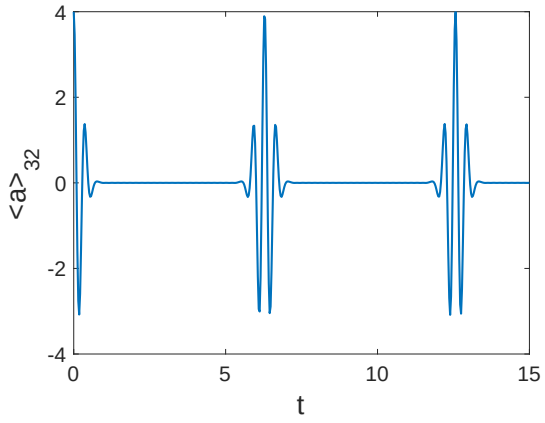

Figure 4. Anharmonic evolution of a coherent phase state mean amplitude, $\langle\hat{a}\rangle$, for an initial state with $\alpha_0 = 4$ and $d = 32$. The graph shows the CPS numerical solution, which is indistinguishable from an analytic calculation with no cutoff.

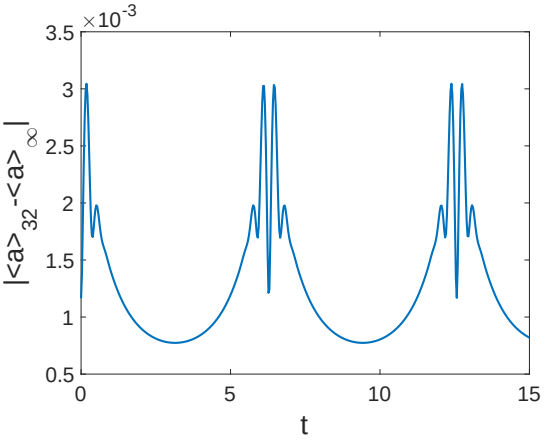

Figure 5. Change in the mean amplitude, $\langle\hat{a}\rangle$, for anharmonic evolution of initial coherent state using CPS states with $\alpha_0 = 4$ and $d = 32$, showing the effects of the CPS number cutoff.

the unitary matrix U includes a nonlinear Hamiltonian $H_n = \kappa(\hat{n} - n_m/2)^2/2$, together with a renormalized linear detuning of $\tilde{\omega} = \omega + \kappa n_m/2$. As expected, using the hybrid picture makes little or no difference: both forms are equally exact.

In this calculation, there is also a 50% larger cutoff of $d = 3\alpha^2 = 48$. The maximum difference is now reduced to 1.4×10^{-9}. This difference can either be viewed as the difference between an ideal and practical situation, due to a physical limit to the photon number from saturation effects. Alternatively the difference can be viewed as a numerical artifact of using a number cutoff basis as an approximate representation of a coherent state.

In all cases, computed normalization errors were negligible, at most of order $\sim 10^{-12}$, caused by roundoff in 64 bit IEEE arithmetic and error propagation. This demonstrates that a CPS basis is able to generate accurate results with either type of identity, and with negligible er-

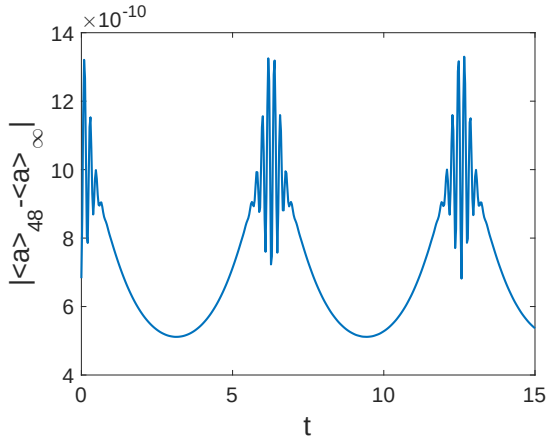

Figure 6. Effects of the number cut-off, for anharmonic evolution of initial coherent state using CPS states with $\alpha_0 = 4$ and $d = 48$, showing reduced discrepancies as small as 10^{-9}.

rors at large cutoff. The advantage is that CPS methods are well suited to complex, multi-mode problems, since the inter-mode coupling between two spatially localized modes is typically linear, with simple coherent identities. These problems will be treated elsewhere.

B. Generation of cat-states and decoherence through phase noise

The anharmonic Hamiltonian Eq. (5.1) has been analyzed by Yurke and Stoler [52] for the purpose of generating Schrödinger cat-states [53] . They denoted the nonlinearity by the symbol $\Omega = \frac{\kappa}{2}$ and solved in the interaction picture without decoherence. After a time $t = t_c = \frac{\pi}{2\Omega}$, a system prepared in a coherent state $|\alpha\rangle$, whereα is real, was shown to evolve to the cat-state

$$|\text{cat}\rangle = \frac{1}{\sqrt{2}}\left(e^{-i\pi/4}|\alpha\rangle + e^{i\pi/4}|-\alpha\rangle\right). \tag{5.4}$$

This macroscopic superposition state is of much interest and for small α has been generated experimentally using different techniques. This is simply the superposition of two coherent states with a relative phase of $\phi = \pi$, and is therefore described exactly in the CPS basis.

However, the time-evolution due to the anharmonic Hamiltonian (5.1) needs to be modified in many real-world situations. For example, the present techniques can be used to treat arbitrary nonlinearities of the form $\hat{n}^p$, by employing the general identities of Eq (3.25).

In ultra-cold atomic physics and photonics, a strong limitation on such experiments is decoherence originating in coupling to external reservoirs. The most common types are losses and/or fluctuating external potentials, which give rise to phase noise. These can be modeled using master equation methods in the limit of broad-band or Markovian reservoirs, or by using the more realistic case of non-Markovian phase-noise. Either - or a combination of both - can be readily solved using projected coherent states.

Since the problem is now dissipative, it is commonly treated using a theory of the full density matrix, $\hat{\rho}$. In the Markovian limit of broad-band phase noise, the resulting master equation has the general Lindblad form:

$$\frac{d\hat{\rho}}{dt} = \frac{1}{i\hbar}\left[\hat{H}_{sys}, \hat{\rho}\right] + \gamma_p(2\hat{n}\hat{\rho}\hat{n} - \hat{n}^2\hat{\rho} - \rho\hat{\rho}\hat{n}) + \gamma_a(2\hat{a}\hat{\rho}\hat{a}^\dagger - \hat{a}^\dagger\hat{a}\hat{\rho} - \hat{\rho}\hat{a}^\dagger\hat{a}) \ . \tag{5.5}$$

The dissipation terms here describe phase decoherence, γ_p and absorptive loss, γ_a, and one can divide the time-evolution into linear and nonlinear parts:

$$\frac{d\hat{\rho}}{dt} = \mathcal{L}^{(n)}\left[\hat{\rho}\right] + \mathcal{L}^{(0)}\left[\hat{\rho}\right] \ . \tag{5.6}$$

where $\mathcal{L}^{(0)}\left[\hat{\rho}\right] = -i\left[\frac{1}{2}\kappa\hat{n}^2, \rho\right]$, and the linear Liouvillian is

$$\mathcal{L}^{(0)}\left[\hat{\rho}\right] = -i\omega\left[\hat{n}, \hat{\rho}\right] + \sum_j \gamma_j(2A_j\hat{\rho}A_j^\dagger - A_j^\dagger A_j\hat{\rho} - \hat{\rho}A_j^\dagger A_j) \ . \tag{5.7}$$

The effects of absorptive loss in the Markovian limit have been treated using the Q-function approach [54]. In this paper we will use our techniques to predict the effect of decoherence in the important case of general, non-Markovian phase noise as opposed to absorptive losses; although both can be included if necessary. With non-Markovian phase-noise, the master equation must be replaced by an average over coherent evolution equations, each with a different fluctuating linear term $\omega(t)$, and functional probability $f[\omega]$.

Yurke and Stoler proposed as a signature for the cat-state the observation of interference fringes in the probability distribution $P(p)$ where p is the result of a measurement of the quadrature phase amplitude $\hat{p} = \frac{1}{i\sqrt{2}}[\hat{a} - \hat{a}^\dagger]$. The probability distribution $P(x)$ for measurement of the orthogonal quadrature $\hat{x} = \frac{1}{\sqrt{2}}[\hat{a} + \hat{a}^\dagger]$ is (for α real) a two-peaked Gaussian, with one hill located at $x = -\sqrt{2}\alpha$ and the other located at $\sqrt{2}\alpha$. The variances $(\Delta x)^2_-$ and $(\Delta x)^2_+$ associated with each hill are given by the variance of a coherent states $|-\alpha\rangle$ and $|\alpha\rangle$: $(\Delta x)^2_\pm = \frac{1}{2}$. As $\alpha \to \infty$, the two hills become macroscopically distinguishable, and there is a simplistic analogy of the " cat" being measured as "alive" or "dead". The two-peaked distribution for $P(x)$ could also be generated by the classical mixture of the two coherent states

$$\rho_{mix} = \frac{1}{2}[|\alpha\rangle\langle\alpha| + |-\alpha\rangle\langle-\alpha|] \tag{5.8}$$

Yurke and Stoler point out that this classical mixture (5.8) however would not give the interference fringes in $P(p)$. The fringes thus distinguish the mixture (5.8) from the superposition (5.4). For α real

$$\langle p|\alpha\rangle = \frac{\exp(-i\sqrt{2}p\alpha + \left[\alpha^2 - p^2 - \|\alpha\|^2\right]/2\}}{\pi^{1/4}} \tag{5.9}$$

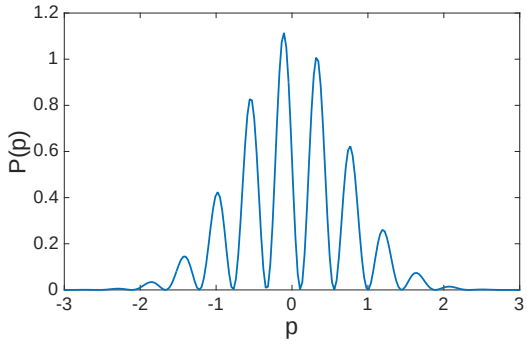

Figure 7. Interference fringes for the anharmonic oscillator at $t = t_c$, $\alpha = 5$.

and hence the distribution for the classical mixture of the coherent states is $P(p) = \frac{1}{\sqrt{\pi}} \exp(-p^2)$, whereas for the superposition it is:

$$P(p) = \frac{e^{-p^2}}{\sqrt{\pi}}[1 - \sin(2\sqrt{2}\alpha p)] \tag{5.10}$$

To evaluate the fringe pattern accounting for the effect of arbitrary phase noise, $\omega(t)$, we note that using the hybrid picture of Eq (3.33), the time-evolution in the CPS basis can be factorized into linear evolution of the reference amplitude $\alpha(t)$, together with a unitary transformation on the discrete phase indices q. The reference amplitude only depends on the time integral of the frequency or accumulated phase

$$\theta(t) = \int_0^t \omega(t')dt'. \tag{5.11}$$

The fringe pattern at the critical time $t = t_c$ is then given by the phase distribution over the accumulated phase $\theta_c = \theta(t_c)$, taking into account that at this time only two CPS states contribute:

$$\begin{aligned} P(p) &= \int f(\theta_c) \left| \sum_q \psi_q \langle p| \left\| \alpha e^{i(q\phi - \theta_c)} \right\rangle_{\mathcal{Q}} \right|^2 d\theta_c \\ &= \frac{1}{2} \int f(\theta_c) \left| \sum_q \psi_q \langle p| \left(|\alpha_c\rangle + i|-\alpha_c\rangle \right) \right|^2 d\theta_c \,, \end{aligned} \tag{5.12}$$

where $\alpha_c = \alpha e^{-i\theta_c}$.

Results obtained using different levels of phase noise are plotted in Figs (7), (8) and (9), with an initial coherent amplitude of $\alpha = 5$, and phase standard deviations of $\sigma = 0$, $\sigma = 0.5$ and $\sigma = 2$ respectively. These results were obtained with a set of 500 points in momentum, and a Gaussian ensemble of 10^5 random phases. They show the destruction and broadening of the fringe pattern due to phase decoherence as the level of phase noise increases.

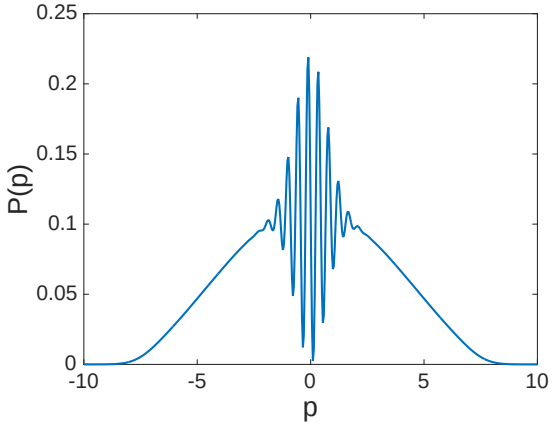

Figure 8. Interference fringes for the anharmonic oscillator at $t = t_c$, $\alpha = 5$, including phase noise with accumulated phase standard deviation of $\sigma = 0.5$.

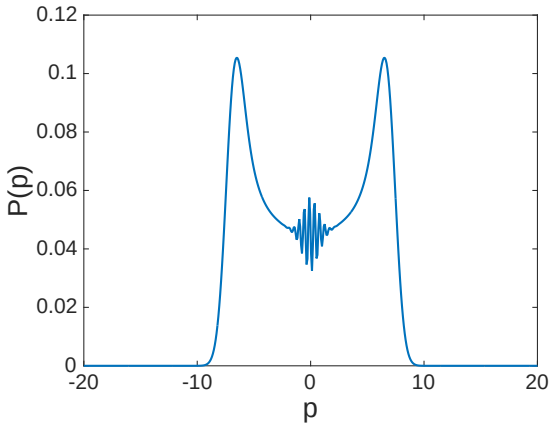

Figure 9. Interference fringes for the anharmonic oscillator at $t = t_c$, $\alpha = 5$, including phase noise with accumulated phase standard deviation of $\sigma = 2.0$.

C. Application to boson sampling and photonic networks

Recent experiments on photonic networks make use of single-photon inputs into a linear, multimode photonic device. A typical experiment excites N input modes of an M mode linear device. This is an M mode beamsplitter, with arbitrary phase-shifts and arbitrary beam-splitting operations. The overall effect is to unitarily transform the M input modes into M output modes. In addition, there are some losses, although these can be modeled as undetected channels.

The output correlations of up to $N-$th order are measured. Well-known results in computational complexity theory indicate that the N-th order correlations, proportional to the square of a matrix permanent, are exponentially hard to compute exactly [55]. It is conjectured that the resulting random samples of photon counts are exponentially complex to generate on a classical com-

puter [56]. This is called the 'Boson Sampling' problem. Other metrology applications of these devices are also being investigated, using interferometric schemes [31].

Phase-space techniques are able to calculate the output correlations very efficiently, although not exactly, owing to the #P hardness of permanents. To achieve this, one must have a representation of the relevant input states. The full contour integral based existence theorem for a arbitrary number state can do this. However, the inputs in many current experiments are binary, with at most a single photon input, so that $n_j = 0, 1$. Such experiments are well suited to the projected P-representation.

Since the initial photon number is bounded, it is useful to consider a projective construction, valid in the limit of $r \to 0$. In this limit the ordinary complex P-representation and the projected complex P-representation are identical, and projected methods allow us to define an alternative existence theorem without changing the basis set. For the qubit case with $n_i = 0, 1$, in each mode and input dimension $d = 2$, one sees from Eq (2.19) that $\phi_i = \{0, \pi\}$, which implies that $\alpha_i = \pm r$.

As explained above, with this expansion, a complex qudit P-function P_Q always exists. In using the small radius limit, all the known identities for the generalized P-representation are all still valid, provided the $r \to 0$ limit is taken after the calculation. Thus, one can use the standard result that after transmission through a linear optical system with phase-shifts, beam-splitters and losses, the only effect on the representation is that the output coherent amplitudes are multiplied by the relevant linear transmission matrix. In calculating $N - th$ order correlations of an $N-$photon input, all the factors proportional to the radius r simply cancel. The advantage of the present approach is that it gives unbiased results for the observable modulus squared of the permanent, and can be readily extended to include more complex inputs, outputs and nonlinear effects.

Complete details and numerical results for boson sampling are given elsewhere [18], showing the qubit basis is particularly useful for treating phase noise effects in boson sampling interferometry in the challenging, large N limit with N up to 100. Because of the exponential hardness of permanent calculations, this is not viable using conventional permanent algorithms above $N = 50$, even on the largest current supercomputers.

VI. CONCLUSION

Results are derived for coherent states in projected spaces. These include the definition of a finite set of coherent phase states, called coherent phase states, which are linearly independent and provide a unique basis for expansions of arbitrary projected states.

These methods allow a new type of generalized P-representation to be introduced, applicable to a projected Hilbert space. Both existence theorems and operator identities applicable to this projected representation are derived. Results are obtained that allow changes of basis.

Calculations are demonstrated with an anharmonic oscillator example, including the effects of phase decoherence on the formation of a Schrödinger cat. As another example, the technique can be readily applied to exponentially complex photonic network experiments.

[1] E. Schrödinger, Naturwissenschaften **14**, 664 (1926).
[2] V. Bargmann, Commun. Pure Appl. Math. **14**, 187 (1961).
[3] R. J. Glauber, Phys. Rev. **131**, 2766 (1963).
[4] S. Chaturvedi, P. Drummond, and D. F. Walls, J. Phys. A **10**, L187 (1977).
[5] P. D. Drummond and C. W. Gardiner, J. Phys. A **13**, 2353 (1980).
[6] R. J. Glauber, Phys. Rev. **131**, 2766 (1963).
[7] E. C. G. Sudarshan, Phys. Rev. Lett. **10**, 277 (1963).
[8] M. Hillery, R. F. O'Connell, M. O. Scully, and E. P. Wigner, Phys. Rep. **106**, 121 (1984).
[9] C. W. Gardiner and P. Zoller, *Quantum Noise*, 2nd ed. (Springer, Berlin, 2000).
[10] P. D. Drummond and S. Chaturvedi, Physica Scripta **91**, 073007 (2016).
[11] P. Deuar and P. D. Drummond, Phys. Rev. Lett. **98**, 120402 (2007).
[12] M. R. Dowling, P. D. Drummond, M. J. Davis, and P. Deuar, Phys. Rev. Lett. **94**, 130401 (2005).
[13] S. Barnett and D. Pegg, Journal of Modern Optics **36**, 7 (1989).
[14] S. M. Barnett and D. B. J., Phys. Scr. **1993**, 13 (1993).
[15] W. K. Wootters, Annals of Physics **176**, 1 (1987).
[16] K. S. Gibbons, M. J. Hoffman, and W. K. Wootters, Physical Review A **70**, 062101 (2004).
[17] S. Chaturvedi, N. Mukunda, and R. Simon, Journal of Physics A: Mathematical and Theoretical **43**, 075302 (2010).
[18] B. Opanchuk, L. E. C. Rosales-Zárate, M. D. Reid, and P. D. Drummond, (2016), arXiv:1609.05614.
[19] T. Aimi and M. Imada, J. Phys. Soc. Jpn. **76**, 113708 (2007).
[20] A. Aspect, P. Grangier, and G. Roger, Phys. Rev. Lett. **47**, 460 (1981).
[21] M. D. Reid, B. Opanchuk, L. Rosales-Zárate, and P. D. Drummond, Phys. Rev. A **90**, 012111 (2014).
[22] L. Rosales-Zárate, B. Opanchuk, P. D. Drummond, and M. D. Reid, Physical Review A **90**, 022109 (2014).
[23] G. Weihs, T. Jennewein, C. Simon, H. Weinfurter, and A. Zeilinger, Phys. Rev. Lett. **81**, 5039 (1998).
[24] S. Aaronson and A. Arkhipov, in *Proceedings of the*

43rd Annual ACM Symposium on Theory of Computing (ACM Press, 2011) pp. 333–342.
[25] S. Aaronson and A. Arkhipov, Theory of Computing **9**, 143 (2013).
[26] M. A. Broome *et al.*, Science **339**, 794 (2013).
[27] A. Crespi *et al.*, Nat. Photon. **7**, 545 (2013).
[28] M. Tillmann *et al.*, Nat. Photon. **7**, 540 (2013).
[29] J. B. Spring *et al.*, Science **339**, 798 (2013).
[30] J. L. O'Brien, A. Furusawa, and J. Vuckovic, Nat. Photon. **3**, 687 (2009).
[31] K. R. Motes *et al.*, Phys. Rev. Lett. **114**, 170802 (2015).
[32] A. D. Corcoles, E. Magesan, S. J. Srinivasan, A. W. Cross, M. Steffen, J. M. Gambetta, and J. M. Chow, Nat Commun **6** (2015).
[33] M. Eichenfield, R. Camacho, J. Chan, K. J. Vahala, and O. Painter, Nature **459**, 550 (2009).
[34] W. S. Bakr, J. I. Gillen, A. Peng, S. Fölling, and M. Greiner, Nature **462**, 74 (2009).
[35] R. J. Glauber, Physical Review Letters **10**, 84 (1963).
[36] R. J. Glauber, Phys. Rev. **130**, 2529 (1963).
[37] D. Zwillinger, *Table of integrals, series, and products* (Elsevier, 2014).
[38] K. A. Dennison and W. K. Wootters, Phys. Rev. A **65**, 010301 (2001).
[39] A. M. Perelomov, Comm. Math. Phys. **26**, 222 (1972).
[40] A. M. Perelomov, *Generalized coherent states and their applications*, Texts and monographs in physics (Springer, Berlin, 1986).
[41] W.-M. Zhang, D. H. Feng, and R. Gilmore, Rev. Mod. Phys. **62**, 867 (1990).
[42] Arvind, N. Mukunda, and R. Simon, J. Phys. A **31**, 565 (1998).
[43] D. W. Barry and P. D. Drummond, Phys. Rev. A **78**, 052108 (2008).
[44] S. Chaturvedi, G. S. Agarwal, and V. Srinivasan, J. Phys. A **27**, L39 (1994).
[45] P. D. Drummond and C. W. Gardiner, J. Phys. A: Math. Gen. **13**, 2353 (1980).
[46] P. D. Drummond and M. Hillery, *The Quantum Theory of Nonlinear Optics* (Cambridge University Press, 2014).
[47] P. Deuar and P. D. Drummond, Phys. Rev. A **66**, 033812 (2002).
[48] P. Deuar and P. D. Drummond, J. Phys. A **39**, 1163 (2006).
[49] P. Deuar and P. D. Drummond, J. Phys. A **39**, 2723 (2006).
[50] G. J. Milburn, Phys. Rev. A **33**, 674 (1986).
[51] M. Greiner, O. Mandel, T. W. Hansch, and I. Bloch, Nature **419**, 51 (2002).
[52] B. Yurke and D. Stoler, Physical review letters **57**, 13 (1986).
[53] E. Schrödinger, Naturwissenschaften **23**, 823 (1935).
[54] G. J. Milburn and C. A. Holmes, Phys. Rev. Lett. **56**, 2237 (1986).
[55] L. Valiant, Theoretical Computer Science **8**, 189 (1979).
[56] S. Aaronson, Proceedings of the Royal Society of London A: Mathematical, Physical and Engineering Sciences **467**, 3393 (2011).